

## CT Angiography with Electrocardiographically Gated Reconstruction for Visualizing Pulsation of Intracranial Aneurysms: Identification of Aneurysmal Protuberance Presumably Associated with Wall Thinning

Motoharu Hayakawa, Kazuhiro Katada, Hirofumi Anno, Shuei Imizu, Junichi Hayashi, Keiko Irie, Makoto Negoro, Yoko Kato, Tetsuo Kanno, and Hirotohi Sano

**Summary:** Electrocardiographically (ECG) gated multisection helical CT images were obtained in 23 patients with ruptured intracranial aneurysms. 4D-CTA (3D CT angiography plus phase data) images were generated by ECG-gated reconstruction. Four patients showed pulsation of an aneurysmal bleb. Clipping was performed in two of these patients, and the rupture site matched the pulsatile bleb seen in 4D-CTA.

The risk factors for rupture of the aneurysm that have been reported are the size of the aneurysm, hypertension, smoking, and the presence of multiple lesions (1–3), and the only risk factor related to the aneurysm itself is its size (10 mm or larger; 3). Although the size of the aneurysm has been shown to be a definite risk factor, it has a low predictive value.

In the present study, we employed electrocardiographically (ECG) gated image acquisition and ECG-gated reconstruction of ruptured intracranial aneurysms, visualized pulsation of the aneurysms, and compared the images against surgical findings.

### Subjects

One hundred ninety-two patients with ruptured aneurysms were treated at our hospital between June 2001 and October 2003. Twenty-three of these patients were randomly selected to undergo 4D-CTA (3D CT angiography plus phase data) examination. They included 7 men and 16 women ranging in age from 24 to 89 years (mean age, 57.0 years). The ruptured intracranial aneurysm was <11 mm in diameter in 20 patients, 11–25 mm in two patients, and 25 mm or more in one patient. The location was the interior carotid artery-posterior communicating artery (IC-PC) in six patients, the middle cerebral artery (MCA) in eight patients, the anterior communicating artery in five patients, the basilar artery tip in two patients, the IC-

bifurcation in one patient, and the vertebral artery (VA) in one patient (Table).

### Imaging Conditions

CT angiographic images of the region around the circle of Willis were acquired by using multisection helical CT systems (Aquilion 4-, 8-, and 16-row multisection helical CT scanners; Toshiba Medical Systems, Tokyo, Japan) in ECG-gated mode with a tube current of 260 mA and a tube voltage of 135 kV. The helical pitch/tube rotation speed was 0.7–1.2/0.4 seconds per rotation with the 4-row system in seven patients, 2.0–2.4/0.4 or 0.5 seconds per rotation with the 8-row system in six patients, and 2.0–4.0/0.4–0.6 seconds per rotation with the 16-row system in 10 patients. Images were reconstructed by using the ECG-gated reconstruction method (with the R-R interval divided into 20 phases at 5% intervals) (Fig 1).

A total of 100 mL of the nonionic contrast medium iopamidol at an iodine concentration of 370 mgI/mL (Iopamiron 370; Schering, Osaka, Japan) was injected intravenously at a rate of 3 mL/s by using an automatic injector. Scanning was started after a delay time of 20–23 seconds following the start of injection or by using the bolus-tracking function (SureStart; Toshiba) of the CT scanner.

### ECG-Gated Reconstruction Method

ECG-gated reconstruction is a method for minimizing cardiac motion artifacts by performing scanning while monitoring the ECG. It has conventionally been employed for reconstruction in electron-beam CT fast imaging of the coronary arteries, which are strongly affected by cardiac motion (4). Recently, however, helical CT has enjoyed an increase in tube rotation speed and the introduction of multisection technology, making it possible to employ the ECG-gated reconstruction method to minimize cardiac motion artifacts in imaging of the coronary arteries and the aortic arch (5).

There are two ECG-gated reconstruction methods: the half-reconstruction method and the segmental reconstruction method. In the former method, the temporal resolution can be improved irrespective of the beam pitch. The latter method can also be used to improve the temporal resolution, but it suffers from limitations with regard to helical pitch, tube rotation speed, and heart rate.

In the present study, half-reconstruction and segmental reconstruction were employed in combination to improve the temporal resolution in image processing. One cardiac cycle was divided into 20 phases, and the images were processed.

Received November 5, 2004; accepted after revision January 26, 2005.

From the Departments of Neurosurgery (M.H., S.I., J.H., K.I., M.N., Y.K., T.K., H.S.) and Radiology (K.K.), School of Medicine, and the Faculty of Radiological Technology (H.A.), School of Health Sciences, Fujita Health University, Aichi, Japan.

Address correspondence to Motoharu Hayakawa, Department of Neurosurgery, School of Medicine, Fujita Health University, 1-98 Dengakugakubo, Kutukake, Toyoake, Aichi 470-1192, Japan.

## Location and size of aneurysms

| Location           | Size   |          |        |
|--------------------|--------|----------|--------|
|                    | <11 mm | 11–25 mm | ≥25 mm |
| IC-PC              | 6      |          |        |
| MCA M1-M2 junction | 5      | 2        |        |
| MCA M1 segment     |        |          | 1      |
| A-com              | 5      |          |        |
| IC-bifurcation     | 1      |          |        |
| BA-tip             | 2      |          |        |
| VA                 | 1      |          |        |

Note.—IC-PC indicates Internal carotid artery–posterior communicating artery; MCA, Middle cerebral artery; A-com, Anterior communicating artery; IC-bifurcation, Internal carotid artery bifurcation; BA-tip, Basilar artery tip; VA, Vertebral artery.

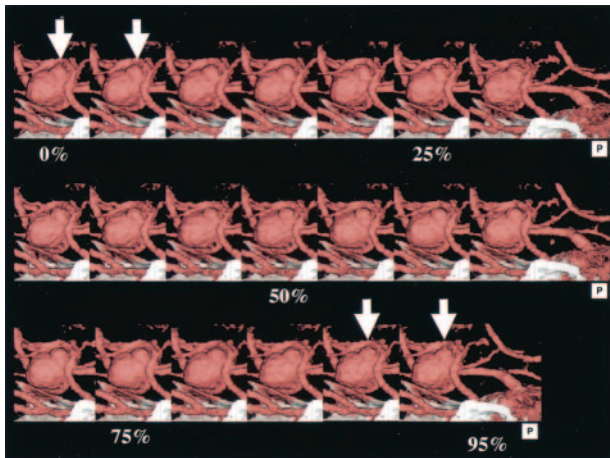


FIG 1. 3D-CT angiography of large intracranial aneurysm of the left MCA. The aneurysm with an associated bleb is seen at the origin of the left MCA (arrow).

## Detection of Pulsation

Pulsation was considered to be present when a protuberance was continuously observed on a part of the aneurysm over three or more phases, with this finding seen only once during a single cardiac cycle. The decision of whether pulsation was present was made by two radiologists and one neurosurgeon. They reviewed the 4D-CTA data of the aneurysms as a group. The aneurysms were displayed as movies and sequential images.

## Results

Acceptable contrast enhancement was achieved in all 23 patients, and the quality of the acquired dynamic 4D-CTA images was judged to be acceptable for image interpretation (Figs 2 and 3). In ECG-gated reconstruction, a small protuberance in the aneurysmal bleb was observed in two patients during the period from 90% to 5% of the R-R interval (Figs 1 and 4), in one patient during the period from 45% to 55% of the R-R interval (Fig 5), and in one patient during the period from 55% to 70% of the R-R interval. In helical scanning, each section contained small artifacts related to helical scanning at the time of reconstruction, thus showing discontinuous movement that was not synchronized with the heart rate. These findings were regarded as negative.

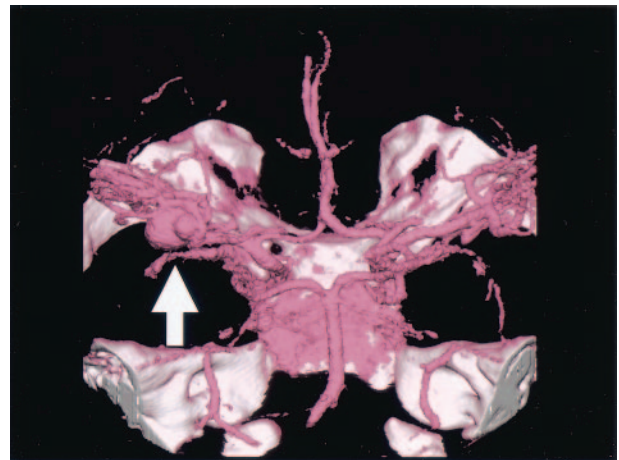


FIG 2. 4D-CT angiography of large intracranial aneurysm of the left MCA, showing ECG-gated reconstruction of an intracranial aneurysm of the left MCA. The cardiac cycle was divided into 20 phases at 5% increments. During the period from 90% to 5% of the R-R interval, a small protuberance appeared at the bleb (arrow).

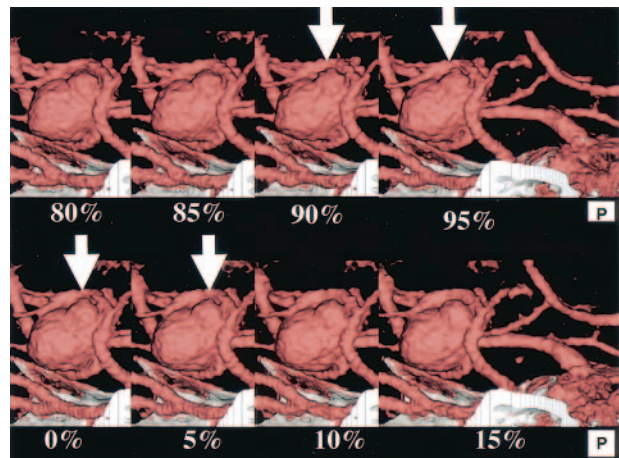


FIG 3. 3D-CT angiography of intracranial aneurysm of the right MCA. The aneurysm with an associated bleb is seen at the origin of the right MCA (arrow).

Clipping was performed in two of the four patients in whom pulsation was observed. During surgery, the intracranial aneurysm was exposed after clipping of the neck, and the rupture site was found to be identical to the area of the bleb where pulsation was observed by 4D-CTA (Figs 6 and 7). The remaining two patients underwent embolization of the intracranial aneurysm by GDC coil placement.

## Discussion

In the cardiac cycle, systole corresponds to the period from 0% to 50% of the R-R interval, with maximum contraction occurring at approximately 25%. The pulse wave generated during systole propagates toward the periphery at a speed of 4–6 m/s in the aorta and 8–12 m/s in the muscular arteries (6). In the present study, pulsation of intracranial aneurysms was observed during the period from 45% to 55%,



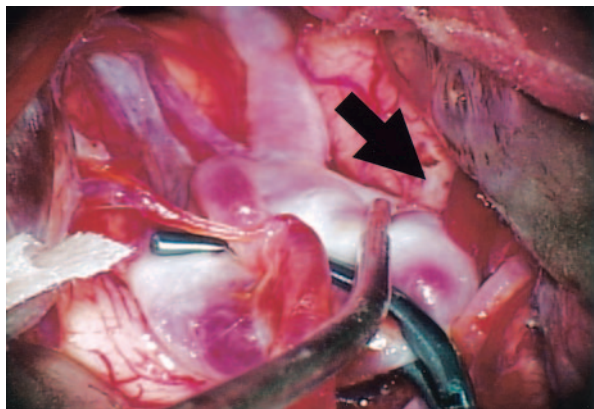


FIG 4. 4D-CT angiography of large intracranial aneurysm of the left MCA. Detail of Figure 1, 80–95%, 0–15%. A small protuberance from the bleb is seen during the period from 90% to 5% of the R-R interval (arrow).

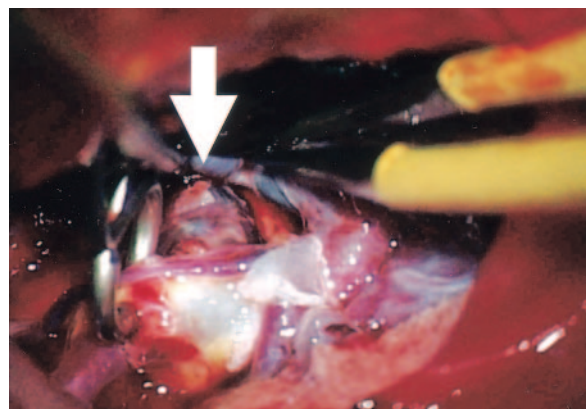


FIG 7. Operation view of right MCA aneurysm. Intracranial aneurysm of the right MCA was clipped. The ruptured aneurysmal bleb is identified (arrow).

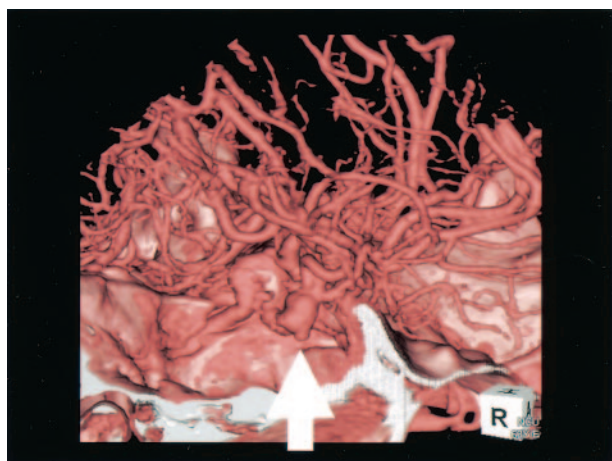


FIG 5. 4D-CT angiography of intracranial aneurysm of the right MCA. A small protuberance from the bleb is seen during the period from 45% to 55% of the R-R interval (arrow).

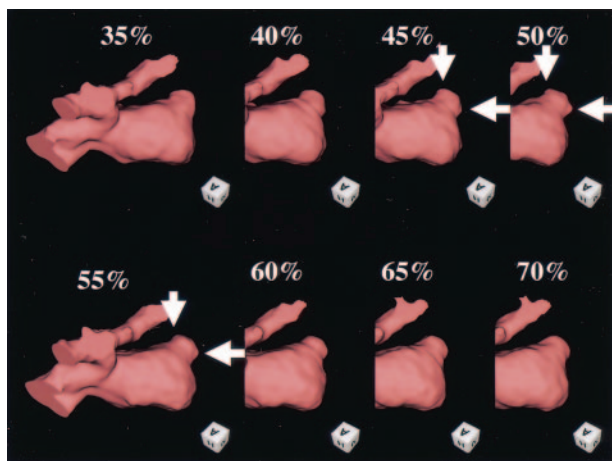


FIG 6. Operation view of left MCA large aneurysm. Intracranial aneurysm of the left MCA was clipped partially. The aneurysmal wall thinning is identified (arrow).

55% to 70%, or 90% to 5% of the R-R interval, depending on the particular case. It is therefore important to obtain a clearer understanding of the prop-

agation of the pulse wave into intracranial aneurysms. In addition, because the cerebral blood vessels are relatively unaffected by cardiac motion, to the best of our knowledge, there have been no studies in which this reconstruction method was employed for the visualization of ruptured intracranial aneurysms.

In the pathologic assessment of ruptured intracranial aneurysms, it has been reported that 84% of aneurysms rupture in the dome, 14% in the wall, and 2% in the neck (7). In particular, the presence of a bleb is important as an indication of the rupture site. The results of the present study showed that pulsation was observed only in a bleb on the aneurysmal dome. Two patients underwent clipping, and it was found that the rupture site exactly matched the location of the pulsatile bleb observed by 4D-CTA. Therefore, the location of the pulsatile bleb accurately indicated the rupture site. Several reports have suggested that the presence of a bleb is indicative of a high risk of bleeding (8, 9). In both of our two cases, radiologic and intraoperative observation indicated the same location.

At the present time, the ability to detect pulsation in ruptured intracranial aneurysms is limited (4/23). An increase in the number of detectors, a reduction in helical artifacts, and improvements in reconstruction functions are needed to enhance the ability to detect aneurysmal pulsation.

With regard to unruptured intracranial aneurysms, a number of risk factors for rupture have been identified, and the treatment protocol for unruptured intracranial aneurysms is based on these factors; however, the only risk factor for rupture that is related to the aneurysm itself is its size (1–3). Moreover, many unruptured/ruptured intracranial aneurysms are small (3, 10). Meyer et al employed MR angiography to identify the structural weakness in the aneurysmal wall (11). We detected pulsation in the bleb of ruptured intracranial aneurysms, and the area of pulsation was found to agree with the rupture site.

**Conclusion**

In this study, we observed aneurysmal pulsation in four of 23 patients with ruptured intracranial aneu-

rysms. In two of the patients who underwent surgical clipping, the site of pulsation was correlated with the site of rupture. The significance of observing aneurysmal pulsation in imaging studies remains to be determined.

### References

1. Juvela S, Porras M, Poussa K. **Natural history of unruptured intracranial aneurysms: probability of and risk factors for aneurysm rupture.** *J Neurosurg* 2000;93:379–387
2. Yasui N, Suzuki A, Nishimura H, et al. **Long-term follow-up study of unruptured intracranial aneurysms.** *Neurosurg* 1997;40:1155–1160
3. Kassell NF, Torner JC, Haley EC Jr, et al. **The International Cooperative Study on the Timing of Aneurysm Surgery. Part 1. Overall management results.** *J Neurosurg* 1990;73:37–47
4. Moshage WEL, Achenbach S, Seese B, et al. **Coronary artery stenosis: three-dimensional imaging with electrocardiographically triggered, contrast agent-enhanced, electron-beam CT.** *Radiology* 1995;196:707–714
5. Ohnesorge B, Flohr T, Becker C, et al. **Cardiac imaging by means of electrocardiographically gated multisection spiral CT: initial experience.** *Radiology* 2000;217:564–571
6. Schmidt RF, Thews G. *The arterial part of the systemic circulation: human physiology.* Berlin: Springer-Verlag;1983:407–413
7. Weir B, Macdonald RL. **214 intracranial aneurysms and subarachnoid hemorrhage: an overview.** In: Wilkins RH, Rengachary SS, eds. *Neurosurgery.* 2nd ed. McGraw-Hill, 1996:2191–2213
8. Frerichs KU, Stieg PE, Friedlander RM. **Prediction of aneurysm rupture site by an angiographically identified bleb at the aneurysm neck.** *J Neurosurg* 2000;93:517
9. Nakase H, Aketa S, Sakaki T, et al. **Detection of a newly developed thin-walled out pouching (“bleb”) in an unruptured intracranial aneurysm by computed tomographic angiography.** *Acta Neurochir (Wien)* 1998;140:517–518
10. Rinkel GJ, Djibuti M, Algra A, van Gijn J. **Prevalence and risk of rupture of intracranial aneurysms: a systemic review.** *Stroke* 1998;29:251–256
11. Meyer FB, Huston J 3rd, Riederer SS. **Pulsatile increases in aneurysm size determined by cine phase-contrast MR angiography.** *J Neurosurg* 1993;78:879–883